Correlation Effects in Diffusion of CH_4/CF_4 Mixtures in MFI Zeolite. A Study Linking MD Simulations with the Maxwell−Stefan Formulation

Anastasios I. Skoulidas,† David S. Sholl,† and Rajamani Krishna*,‡

Department of Chemical Engineering, Carnegie Mellon University, Pittsburgh, Pennsylvania 15213, and Department of Chemical Engineering, University of Amsterdam, Nieuwe Achtergracht 166, 1018 WV Amsterdam, The Netherlands

Received May 3, 2003. In Final Form: July 2, 2003

Correlation effects in diffusion of CH_4 and CF_4 in MFI zeolite have been investigated with the help of molecular dynamics (MD) simulations and the Maxwell−Stefan (M−S) formulation. For single-component diffusion, the correlations are captured by the self-exchange coefficient $Đ_{ii}^{corr}$; in the published literature this coefficient has been assumed to be equal to the single-component M−S diffusivity, $Đ_i$. A detailed analysis of single-component diffusivity data from MD, along with published kinetic Monte Carlo (KMC) simulations, reveals that $Đ_{ii}^{corr}/Đ_i$ is a decreasing function of the molecular loading, depends on the guest−host combination, and is affected by intermolecular repulsion (attraction) forces. A comparison of published KMC simulations for diffusion of various molecules in MFI, with those of primitive square and cubic lattices, shows that the self-exchange coefficient increases with increasing connectivity. Correlations in CH_4/CF_4 binary mixtures are described by the binary exchange coefficient $Đ_{12}^{corr}$; this exchange coefficient has been examined using Onsager transport coefficients computed from MD simulations. Analysis of the MD data leads to the development of a logarithmic interpolation formula to relate $Đ_{12}^{corr}$ with the self-exchange coefficient $Đ_{ii}^{corr}$ of the constituents. The suggested procedure for estimation of $Đ_{12}^{corr}$ is validated by comparison with MD simulations of the Onsager and Fick transport coefficients for a variety of loadings and compositions. Our studies show that a combination of the M−S formulation and the ideal adsorbed solution theory allows good predictions of binary mixture transport on the basis of only pure component diffusion and sorption data.

1. Introduction

Zeolites are widely used as catalysts and adsorbents in a variety of applications in the process industries.[1] For reliable design of catalytic reactors, adsorbers, and membrane permeation devices employing zeolites, it is necessary to estimate the intracrystalline diffusion coefficients. For multicomponent mixtures usually encountered in practice, the transport or Fick diffusivities are required; for *n*-component diffusion, these are *defined* by the *n*-dimensional matrix relation

$$(\mathbf{N}) = -\rho[D](\nabla\Theta) \tag{1}$$

where $\mathbf{N}_i$ is the flux of species *i* expressed, say, in molecules per square meter per second, Θ_i is the loading in molecules per unit cell; D_{ik} are the Fick diffusivities with the units square meter per second, and ρ is the zeolite density expressed as the number of unit cells per cubic meter. The Fick diffusivity matrix [*D*] usually has sizable off-diagonal elements, and therefore, the individual fluxes $\mathbf{N}_i$ are strongly *coupled* to one another. The Fick diffusivities are strong functions of the molecular loadings Θ_i; these, in turn, are determined by the multicomponent sorption characteristics. Diffusion and sorption phenomena are inextricably linked to each other.

While there are several studies on measurement of transport diffusivities of single species within a zeolite,[1,2] there are far fewer studies reporting [*D*] values for multicomponent, even binary, mixtures.[3−5] Other experimental works have reported transient uptake of binary mixtures in zeolite crystals[6,7] but have not extracted values of the elements of [*D*]. A few experimental studies have reported self-diffusivities, $D_{i,self}$, in binary mixtures;[8−10] these diffusivities are insufficient in themselves to provide information on [*D*].

In recent years, molecular simulation techniques have been used with considerable success to study both sorption and diffusion in zeolites.[11−14] Grand canonical Monte Carlo (GCMC) and configurational-bias Monte Carlo (CBMC) simulations have been used to calculate sorption isotherms of single components and mixtures in a variety of zeolites.[15−18] Transition-state theory (TST) has been used

* Fax: + 31 20 5255604. E-mail: krishna@science.uva.nl.
† Carnegie Mellon University.
‡ University of Amsterdam.

(1) Kärger, J.; Ruthven, D. M. *Diffusion in zeolites and other microporous solids*; John Wiley: New York, 1992.
(2) Ruthven, D. M.; Post, M. F. M. Diffusion in zeolite molecular sieves. In *Introduction to Zeolite Science and Practice*, 2nd ed.; van Bekkum, H., Flanigan, E. M., Jacobs, P. A., Jansen, J. C., Eds.; Elsevier: Amsterdam, 2001; Vol. 137, Chapter 12, p 525.
(3) Kärger, J.; Bülow, M.; Schirmer, W. *Z. Phys. Chem. (Leipzig)* **1975**, *256*, 144.
(4) Carlson, N. W.; Dranoff, J. S. Competitive adsorption of methane and ethane on 4A zeolite. In *Fundamentals of Adsorption*; Liapis, A. I., Ed.; AIChE: New York, 1986; p 129.
(5) Yasuda, Y.; Matsumoto, K. *J. Phys. Chem.* **1989**, *93*, 3195.
(6) Qureshi, W. R.; Wei, J. *J. Catal.* **1990**, *126*, 147.
(7) Karge, H. G.; Niessen, W. *Catal. Today* **1991**, *8*, 451.
(8) Snurr, R. Q.; Kärger, J. *J. Phys. Chem. B* **1997**, *101*, 6469.
(9) Gergidis, L. N.; Theodorou, D. N.; Jobic, H. *J. Phys. Chem. B* **2000**, *104*, 5541.
(10) Schuring, D.; Koriabkina, A. O.; de Jong, A. M.; Smit, B.; van Santen, R. A. *J. Phys. Chem. B* **2001**, *105*, 7690.
(11) Auerbach, S. M. *Int. Rev. Phys. Chem.* **2000**, *19*, 155.
(12) Smit, B.; Krishna, R. *Chem. Eng. Sci.* **2003**, *58*, 557.
(13) Fuchs, A. H.; Cheetham, A. K. *J. Phys. Chem. B* **2001**, *105*, 7375.
(14) Keil, F. J.; Krishna, R.; Coppens, M. O. *Rev. Chem. Eng.* **2000**, *16*, 71.
(15) Skoulidas, A. I.; Sholl, D. S. *J. Phys. Chem. B* **2001**, *105*, 3151.
(16) Skoulidas, A. I.; Sholl, D. S. *J. Phys. Chem. B* **2002**, *106*, 5058.

10.1021/la034759a CCC: $25.00
Published on Web 08/08/2003

to calculate the zero-loading diffusivities of single components.[19,20] Molecular dynamics (MD) and kinetic Monte Carlo (KMC) simulations have been used to determine transport and self-diffusivities in single components[15,16,21−24] and in binary mixtures,[8,25−29] as a function of the molecular loading. MD simulation studies of [$Đ$] in binary mixtures of CH_4/CF_4 in Faujasite[25,26] and in silicalite-1 (MFI topology)[27] have emphasized the strong variation with loadings and composition. No attempt was made in this prior work, however, to relate the elements of [$Đ$] to the *single*-component transport and sorption.

From a practical equipment design viewpoint, we would like to have the capability of *predicting* the elements of [$Đ$] using only information on the *single*-component sorption and diffusion. The Maxwell−Stefan (M−S) formulation for zeolite diffusion[30−32] provides a framework for the development of such a predictive method. In the M−S formulation, entirely consistent with the theory of irreversible thermodynamics, the chemical potential gradients are written as linear functions of the fluxes:[28,30−34]

$$-\rho\frac{\theta_i}{RT}\nabla\mu_i = \sum_{\substack{j=1\\ j\neq i}}^{n}\frac{\Theta_j\mathbf{N}_i - \Theta_i\mathbf{N}_j}{\Theta_{i,\mathrm{sat}}\Theta_{j,\mathrm{sat}}Đ_{ij}^{\mathrm{corr}}} + \frac{\mathbf{N}_i}{\Theta_{i,\mathrm{sat}}Đ_i}; \quad i = 1, ..., n \tag{2}$$

where $\Theta_{i,\mathrm{sat}}$ represents the saturation loading of species i and n is the total number of diffusing species. The fractional occupancies θ_i are defined by

$$\theta_i \equiv \Theta_i/\Theta_{i,\mathrm{sat}} \qquad i = 1, 2, ..., n \tag{3}$$

To use eq 2 we have to define two types of M−S diffusivities: $Đ_i$ and $Đ_{ij}^{\mathrm{corr}}$. If we have only a single sorbed component, then only one $Đ_i$ is needed, and in this case, it is equivalent to the single-component "corrected" diffusivity.[15] In the case of mixture diffusion, the $Đ_i$ values depend, in general, on the loading of all sorbed species, so $Đ_i = Đ_i(\Theta_1,\Theta_2,...,\Theta_n)$. The exchange coefficients $Đ_{ij}^{\mathrm{corr}}$ reflect *correlation* effects in mixture diffusion. Site-to-site jump leaves behind a vacancy (cf. the pictorial representation in Figure 1 of jumps in the MFI zeolite topology), and subsequent jumps are more likely to fill this vacancy, thus producing "vacancy correlation" effects.[35] Correlation effects of this type can also arise due to anisotropy of the particular zeolite topology. Correlation effects in either single-component or mixture diffusion can also arise due to momentum transfer between sorbed molecules[16] or from concerted motions of clusters of sorbed molecules.[36−39] For a clear discussion on correlation effects in diffusion, we refer the reader to the recent review by Kärger et al.[19] For mixture diffusion the $Đ_{ij}^{\mathrm{corr}}$ tends to slow the more mobile species and speed up the relatively sluggish ones. A lower value of the exchange coefficient $Đ_{ij}^{\mathrm{corr}}$ implies a *stronger* correlation effect. When $Đ_{ij}^{\mathrm{corr}} \rightarrow \infty$, correlation effects vanish; we shall call this the *facile exchange* scenario.

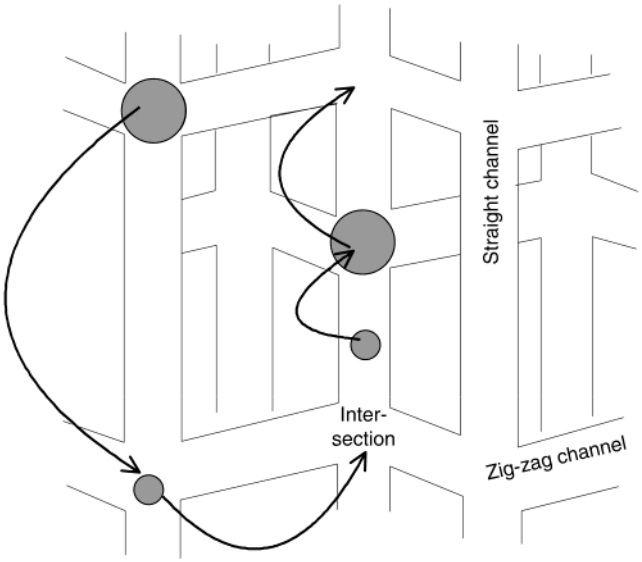

Figure 1. Pictorial representation of the molecular jumps in MFI topology. Molecules jump from one site to another site that is either vacant or recently vacated by another molecule. Smaller, more mobile, molecules tend to vacate their sites more frequently, effectively speeding up larger sluggish species. On the other hand, the larger sluggish molecules are tardy in vacating a site, thus effectively slowing down the faster species.

Defining an n-dimensional square matrix [B] with elements

$$B_{ii} = \frac{1}{Đ_i} + \sum_{\substack{j=1\\ j\neq i}}^{n}\frac{\theta_j}{Đ_{ij}^{\mathrm{corr}}}; \quad B_{ij} = -\frac{\theta_i}{Đ_{ij}^{\mathrm{corr}}}; \quad i, j = 1, 2, ..., n \tag{4}$$

allows us to recast eq 2 into n-dimensional matrix notation as

$$(\mathbf{N}) = -\rho[B]^{-1}[\Gamma](\nabla\Theta) \tag{5}$$

where the matrix of thermodynamic correction factors [Γ], defined by

$$\frac{\theta_i}{RT}\nabla\mu_i = \sum_{j=1}^{n}\Gamma_{ij}\nabla\theta_j; \quad \Gamma_{ij} \equiv \left(\frac{\Theta_{j,\mathrm{sat}}}{\Theta_{i,\mathrm{sat}}}\right)\frac{\Theta_i}{p_i}\frac{\partial p_i}{\partial\Theta_j} \equiv \frac{\theta_i}{\theta_j}\frac{\partial \ln p_i}{\partial \ln \theta_j}; \quad i, j = 1, ..., n \tag{6}$$

can be calculated from knowledge of the multicomponent sorption isotherms. Comparing eqs 1 and 5, we obtain an explicit expression for the Fick matrix:

(17) Vlugt, T. J. H.; Krishna, R.; Smit, B. *J. Phys. Chem. B* **1999**, *103*, 1102.
(18) Krishna, R.; Smit, B.; Calero, S. *Chem. Soc. Rev.* **2002**, *31*, 185.
(19) Kärger, J.; Vasenkov, S.; Auerbach, S. M. Diffusion in zeolites. In *Handbook of Zeolite Science and Technology*; Auerbach, S. M., Carrado, K. A., Dutta, P. K., Eds.; Marcel Dekker: New York, 2003; Chapter 10.
(20) Vlugt, T. J. H.; Dellago, C.; Smit, B. *J. Chem. Phys.* **2000**, *113*, 8791.
(21) Coppens, M. O.; Bell, A. T.; Chakraborty, A. K. *Chem. Eng. Sci.* **1999**, *54*, 3455.
(22) Maginn, E. J.; Bell, A. T.; Theodorou, D. N. *J. Phys. Chem.* **1993**, *97*, 4173.
(23) Paschek, D.; Krishna, R. *Phys. Chem. Chem. Phys.* **2000**, *2*, 2389.
(24) Paschek, D.; Krishna, R. *Chem. Phys. Lett.* **2001**, *342*, 148.
(25) Sanborn, M. J.; Snurr, R. Q. *Sep. Purif. Technol.* **2000**, *20*, 1.
(26) Sanborn, M. J.; Snurr, R. Q. *AIChE J.* **2001**, *47*, 2032.
(27) Skoulidas, A. I.; Bowen, T. C.; Doelling, C. M.; Falconer, J. L.; Noble, R. D.; Sholl, D. S. *J. Membr. Sci.*, in press.
(28) Paschek, D.; Krishna, R. *Phys. Chem. Chem. Phys.* **2001**, *3*, 3185.
(29) Maceiras, D. B.; Sholl, D. S. *Langmuir* **2002**, *18*, 7393.
(30) Krishna, R.; Wesselingh, J. A. *Chem. Eng. Sci.* **1997**, *52*, 861.
(31) Kapteijn, F.; Moulijn, J. A.; Krishna, R. *Chem. Eng. Sci.* **2000**, *55*, 2923.
(32) Krishna, R. *Chem. Phys. Lett.* **2002**, *355*, 483.
(33) Krishna, R.; Paschek, D. *Chem. Eng. J.* **2002**, *87*, 1.
(34) Krishna, R.; Paschek, D. *Phys. Chem. Chem. Phys.* **2002**, *4*, 1891.
(35) Fritzsche, S.; Karger, J. *J. Phys. Chem. B* **2003**, *107*, 3515.
(36) Sholl, D. S.; Fichthorn, K. A. *Phys. Rev. Lett.* **1997**, *79*, 3569.
(37) Sholl, D. S. *Chem. Phys. Lett.* **1999**, *305*, 269.
(38) Sholl, D. S.; Lee, C. K. *J. Chem. Phys.* **2000**, *112*, 817.
(39) Sholl, D. S. *Ind. Eng. Chem. Res.* **2000**, *39*, 3737.

$$[D] = [B]^{-1}[\Gamma] \tag{7}$$

The proper estimation of correlation (exchange) coefficients $Đ_{ij}^{corr}$ is a key factor in the prediction of the Fick matrix $[D]$. Krishna and Wesselingh[30] suggested the logarithmic interpolation formula

$$Đ_{ij}^{corr} = [Đ_i]^{\Theta_i/(\Theta_i+\Theta_j)}[Đ_j]^{\Theta_j/(\Theta_i+\Theta_j)} \tag{8}$$

The use of the interpolation formula (eq 8), with the $Đ_i = Đ_i(\Theta_1,\Theta_2)$ estimated from single-component data, has been shown to provide predictions of $[D]$ in good agreement with kinetic Monte Carlo (KMC) simulations of a lattice model of binary and ternary mixtures containing 2-methylhexane (2MH) in MFI, wherein all the species can be located only at the intersections.[28,33] In these simulations the maximum (saturation) loading $\Theta_{i,sat} = 4$ molecules per unit cell for each species and, furthermore, no intermolecular forces are taken into account. Equation 8 can also be used in the prediction of *self*-diffusivities. Previous applications of eq 8 in lattice models of CH_4/CF_4 mixtures produce the proper trends with loading and composition, but there are strong *quantitative* deviations in predictions, especially at high loadings.[29,40] These deviations were caused in part due to the use of a flawed formula for self-diffusion in multicomponent mixtures; a corrected formula has been published subsequently.[34]

The first major objective of the present communication is to obtain a deeper insight into correlation effects and to provide an improved method for estimation of the $Đ_{ij}^{corr}$. Published data on single-component Fick diffusivities, M−S diffusivities, and self-diffusivities taken from atomically detailed simulations[15,16] are used to study correlation effects in the MFI topology. The second major objective is to test the accuracy of the M−S formulation in predicting mixture transport, using only single-component diffusivity and sorption data. Skoulidas et al.[27] have recently presented a detailed study of binary sorption and diffusion of CH_4/CF_4 mixtures in silicalite-1 at 298 K using atomically detailed methods with the aim of describing transport of this mixture through silicalite-1 membranes. We make use of these data to provide stringent tests of the predictive capability of the M−S formulation. We aim to show in the present communication that the estimation procedure for describing correlation effects suggested in earlier publications[29,30,32,34] needs to be refined in order to account for zeolite topology, molecule−molecule repulsions (attractions), and loading effects. Expressions that improve upon eq 8 for approximating mixture exchange coefficients are presented.

2. Atomistic Modeling Details

Because the atomistic simulation data of Skoulidas et al.[15,16,27] on adsorption and diffusion underlies our ability to examine methods for predicting the transport properties of binary mixtures in MFI from single-component information, we review the main features of these data here. The interactions of CH_4 and CF_4 with silicalite-1 were described using Lennard-Jones potentials for adsorbate−adsorbate and adsorbate−zeolite pairs.[15,16,41] Silicalite-1 was assumed to be rigid in its orthorhombic (*Pnma*) form using an experimentally determined crystal structure.[42] Diffusion in silicalite-1 is anisotropic, and for each diffusion coefficient the *x*, *y*, and *z* components were computed separately.[15,16] Below, however, we only consider orientationally averaged diffusivities in which each component is averaged equally.[15,16] All simulations corresponded to adsorption and diffusion at 298 K. Simulations were performed in a simulation volume of at least $2 \times 2 \times 2$ silicalite unit cells. At low adsorbate concentrations, simulation volumes as large as $10 \times 10 \times 10$ unit cells were used to ensure a sufficiently large number of particles for adequate sampling. This atomistic model predicts the CH_4 Henry's law constant, isosteric heat of adsorption, and adsorption isotherms in excellent agreement with experiment.[41,43,44] The CH_4 self-diffusivities calculated with this model are in excellent agreement with PFG-NMR measurements.[43] Agreement between this atomistic model and experimental results for the adsorption isotherm and self-diffusivity of CF_4 is good for low and moderate pore loadings, although minor discrepancies between the model and experiments exist at high loadings.[8,44] Binary adsorption isotherm predictions agree very well with experiments,[44] as do predictions for the binary self-diffusivities, with a slight deviation at high loading.[8]

Single-component and binary adsorption isotherms were computed using grand canonical Monte Carlo (GCMC) simulations. The chemical potential of each component in the bulk gas mixture was related to the partial pressures by a virial equation of state using the second and third mixture coefficients determined experimentally by Doulsin et al.[45] GCMC simulations involved a total of 5×10^6 moves for equilibration and up to 10^8 moves for data collection for each state point.

Adsorbate diffusion coefficients were computed using equilibrium molecular dynamics (EMD). The time steps, equilibration, and convergence procedures for these calculations have been described previously.[27] Self-diffusivities in single-component and binary mixtures were computed by analyzing the mean square displacement of each adsorbate in the usual manner. In addition to the self-diffusivities, it is possible to determine the Onsager coefficients for single-component or binary mixtures from EMD simulations using methods derived by Theodorou et al.[46] The matrix of Onsager transport coefficients $[L]$, defined by

$$(\mathbf{N}) = -[L](\nabla\mu) \tag{9}$$

where $(\nabla\mu)$ is the column matrix of chemical potential gradients, was computed from our EMD simulations using the Einstein form of these methods:

$$L_{ij} = \frac{1}{6Vk_BT}\lim_{\Delta t\to\infty}\frac{1}{\Delta t}\langle(\sum_{l=1}^{N_i}(\mathbf{r}_{l,i}(t+\Delta t) - \mathbf{r}_{l,i}(t)))\cdot(\sum_{k=1}^{N_j}(\mathbf{r}_{k,j}(t+\Delta t) - \mathbf{r}_{k,j}(t)))\rangle \tag{10}$$

In this expression V is the simulation volume, N_i is the number of molecules of species i, and $\mathbf{r}_{l,i}(t)$ is the position of molecule l of species i at any time t. An important feature

(40) Paschek, D.; Krishna, R. *Langmuir* **2001**, *17*, 247.
(41) Bowen, T. C.; Falconer, J. L.; Noble, R. D.; Skoulidas, A. I.; Sholl, D. S. *Ind. Eng. Chem. Res.* **2002**, *41*, 1641.
(42) Olson, D. H.; Kokotailo, G. T.; Lawton, S. L.; Meier, W. M. *J. Phys. Chem.* **1981**, *85*, 2238.
(43) Goodbody, S. J.; Watanabe, K.; MacGowan, D.; Walton, J. R. P. B.; Quirke, N. *J. Chem. Soc., Faraday Trans.* **1991**, *87*, 1951.
(44) Heuchel, M.; Snurr, R. Q.; Buss, E. *Langmuir* **1997**, *13*, 6795.
(45) Doulsin, D. R.; Harrison, R. H.; Moore, R. T. *J. Phys. Chem.* **1967**, *71*, 3477.
(46) Theodorou, D. N.; Snurr, R. Q.; Bell, A. T. Molecular dynamics and diffusion in microporous materials. In *Comprehensive Supramolecular Chemistry*; Alberti, G., Bein, T., Eds.; Pergamon Press: New York, 1996; Vol. 7, p 507.

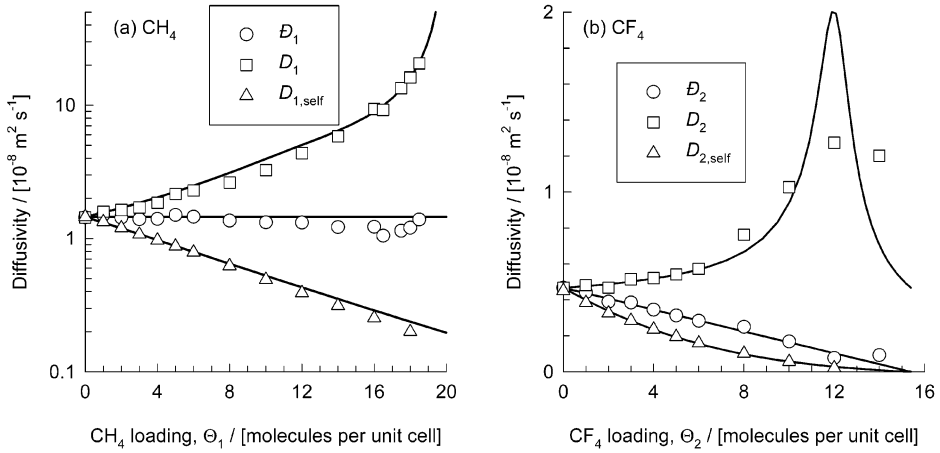

Figure 2. MD simulations (symbols) of M−S diffusivities ($Đ_i$), Fick diffusivities (D_i), and self-diffusivities ($D_{i,self}$) of (a) CH_4 and (b) CF_4, in MFI at 298 K as a function of molecular loading Θ. The MD simulation data are from Skoulidas and Sholl.[16] The continuous lines represent the calculations following either eq 12 or eq 17 for $Đ_i$, eq 13 for D_i, and eq 18 for $D_{i,self}$.

of this method is that it requires data to be averaged over multiple independent EMD trajectories, unlike calculations of the self-diffusivity which can be performed with just a single trajectory of sufficient length. Both the Onsager coefficients and the self-diffusivities for the mixtures considered here were computed using data from 20 independent EMD trajectories at each state point. The Onsager reciprocal relations demand that the matrix [L] be symmetric, that is

$$L_{ij} = L_{ji}; \quad (i \neq j) \tag{11}$$

3. Single-Component Sorption and Diffusion

Figure 2 shows the MD simulations[15,16] for M−S diffusivities ($Đ$), Fick diffusivities (D), and self-diffusivities (D_{self}) of (a) CH_4 and (b) CF_4 adsorbed as single components in silicalite-1 at 298 K as a function of molecular loading Θ. For CH_4, the M−S diffusivity is practically independent of loading and the zero-loading diffusivity, $Đ_1(0) = 1.45 \times 10^{-8}$ m^2/s. Therefore, the M−S diffusivity at any loading can be estimated from

$$Đ_1 = Đ_1(0) \tag{12}$$

Skoulidas and Sholl[16] have found relation 12 to be valid also for diffusion of Ar in silicalite-1; this scenario is typical of *weakly confined* molecules in zeolite hosts. We shall refer to eq 12 as the *weak confinement* scenario.

From the single-component (i) version of eq 7, we can relate the Fick and M−S diffusivities by

$$D_i = Đ_i \Gamma_i \tag{13}$$

with the thermodynamic correction factor Γ

$$\Gamma_i \equiv \frac{\partial \ln p_i}{\partial \ln \Theta_i} \tag{14}$$

The GCMC simulations[15,16] of the single-component sorption isotherms are represented very well with the dual-site (DSL) Langmuir isotherm

$$\Theta_i(P) \equiv \Theta_{i,A} + \Theta_{i,B} = \frac{\Theta_{i,sat,A} b_{i,A} P}{1 + b_{i,A} P} + \frac{\Theta_{i,sat,B} b_{i,B} P}{1 + b_{i,B} P} \tag{15}$$

with the saturation loadings in sites A and B, $\Theta_{i,sat,A}$ and $\Theta_{i,sat,B}$, as specified in Table 1, along with the parameters

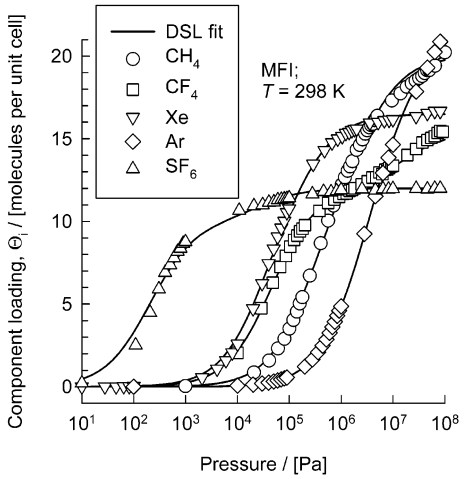

Figure 3. Single-component sorption isotherms for CH_4, CF_4, Ar, Xe, and SF_6 in silicalite-1 at 298 K from GCMC simulations (symbols) of Skoulidas and Sholl.[16] The smooth lines are calculated using the dual-site Langmuir (DSL) parameters listed in Table 1.

Table 1. Dual-Site Langmuir Parameters for Single-Component Silicalite-1 at 298 K, Fitted with the Isotherm Data from Skoulidas and Sholl[16]

	dual Langmuir parameters			
	site A		site B	
component	$b_{i,A}$/Pa^{-1}	$\Theta_{i,sat,A}$/(molecules per unit cell)	$b_{i,B}$/Pa^{-1}	$\Theta_{i,sat,B}$/(molecules per unit cell)
CH_4	3.97×10^{-6}	12.0	3.64×10^{-7}	8.0
CF_4	2.18×10^{-5}	12.0	6.53×10^{-8}	3.4
Ar	4.63×10^{-7}	12.0	1.27×10^{-7}	9.0
Xe	3.06×10^{-5}	12.0	4.86×10^{-6}	4.5
SF_6	4.89×10^{-3}	10.0	3.72×10^{-5}	2.0

$b_{i,A}$ and $b_{i,B}$ (see Figure 3). The total saturation loading for the isotherm in eq 15 is $\Theta_{i,sat} = \Theta_{i,sat,A} + \Theta_{i,sat,B}$.

Carrying out the differentiation in eq 14, we find

$$\Gamma_i = \frac{1}{\frac{\Theta_{i,A}}{\Theta_i}\left(1 - \frac{\Theta_{i,A}}{\Theta_{i,sat,A}}\right) + \frac{\Theta_{i,B}}{\Theta_i}\left(1 - \frac{\Theta_{i,B}}{\Theta_{i,sat,B}}\right)} \tag{16}$$

The Fick diffusivity for a single sorbed species can be determined from MD simulations by directly measuring

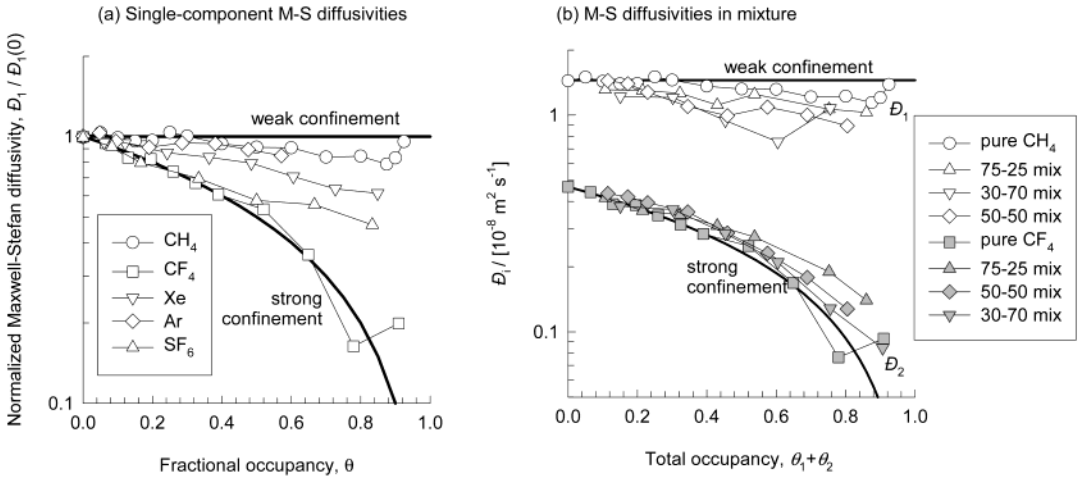

Figure 4. (a) MD simulations (symbols) of M−S diffusivities $Đ_i$ (normalized with respect to zero-loading values) of the *pure* components CH_4, CF_4, Ar, Xe, and SF_6 in MFI at 298 K as a function of fractional occupancy θ. The MD simulation data of Skoulidas and Sholl[16] have been used in conjunction with the $\Theta_{i,sat}$ values obtained from DSL fits of the isotherms (see Figure 3) as specified in Table 1. (b) MD simulations (symbols) of M−S diffusivities $Đ_i$ of CH_4 and CF_4 in 100−0, 75−25, 50−50, 30−70, and 0−100 mixtures. These values are calculated using eq 22. Open (shaded) symbols show the $Đ_i$ of CH_4 (CF_4) in each mixture.

the M−S diffusivity Đ and then using eq 13 to combine this diffusivity Đ with the thermodynamic correction factor Γ defined by the measured isotherm.[15,16] The resulting Fick diffusivity for CH_4 is shown in Figure 2a. Because eq 12 accurately describes the observed M−S diffusivity, predicting the Fick diffusivity using eq 12 yields results in good accord with the data determined directly from the MD simulations.

In contrast to the case of CH_4, the M−S diffusivity for CF_4 shows a strong decrease with increased loading (see Figure 2b). The loading dependence of $Đ_2$ for CF_4 is seen to follow the relation

$$Đ_2 = Đ_2(0)(1 - \Theta_2/\Theta_{2,sat}) = Đ_2(0)(1 - \theta_2) \quad (17)$$

with a zero-loading diffusivity value $Đ_2(0) = 0.467 \times 10^{-8}$ m^2/s. The scenario in eq 17 is typical of *strongly confined* molecules in zeolite hosts. We term eq 17, the *strong confinement* scenario.

The *strong* and *weak* confinement scenarios, depicting the loading (occupancy) dependence of the M−S diffusivity, represent *idealizations* of a variety of dependences that have been observed in practice. To underline this, Figure 4a compares the normalized M−S diffusivity values for CH_4, CF_4, Ar, Xe, and SF_6 determined from MD simulations[16] as a function of the fractional occupancy using the saturation values as determined by the DSL fits of the isotherms (Figure 3) and specified in Table 1. For any particular molecule, its specific occupancy dependency needs to be properly examined and modeled. The specific scenario followed will depend on the *degree of confinement* of the guest−host combination and intermolecular repulsions, or attractions.[47−50] A rough indication of the degree of confinement for a specific host, say MFI, is obtained from the saturation capacity, $\Theta_{i,sat}$. The *lower* the saturation capacity, the *more strongly* confined the molecule, and the $Đ_i/Đ_i(0)$ dependency on θ varies between eqs 12 and 17. It should be noted from Figure 4a that the size of the adsorbate provides only an *approximate* measure of the degree of confinement in the sense discussed above. For example, CF_4 is observed to be more accurately described by the strong confinement scenario than SF_6, although the latter is a larger molecule than the former. Differences in the sorbate−sorbate interactions[47−50] are likely the cause of the differences in the *confinement* scenarios for CF_4 and SF_6.

The sorption isotherm for CF_4 shows an inflection at a loading $\Theta = 12$ (see Figure 3). Consequently, the thermodynamic factor Γ exhibits a maximum at this loading, and this is again reflected in a maximum in the Fick diffusivity D_2, both in the MD simulations and in calculations from eq 13 in which eq 17 is used to estimate the M−S diffusivity (see Figure 2b).

The differences that arise between the M−S $Đ_i$ and the single-component *self*-diffusivity, $D_{i,self}$, are crucially dependent on correlation effects in the diffusing species. This observation can be used to determine the self-exchange coefficient, $Đ_{ii}^{corr}$, provided $Đ_i$ and $D_{i,self}$ are known independently. We will show in section 4 that the self-exchange coefficient $Đ_{ii}^{corr}$ can be very useful in describing *binary* diffusion, so we discuss the behavior of this coefficient for single-component systems here. Essentially, the $Đ_{ii}^{corr}$ values provide a measure of vacancy and geometry correlations[19] for the particular guest−host topology. The *lower* the value of $Đ_{ii}^{corr}$, the *stronger* are the correlation effects. For $Đ_{ii}^{corr} \rightarrow \infty$, correlation effects vanish. Krishna and Paschek[34] have derived the following expression relating $D_{i,self}$ to $Đ_i$ by applying eq 2 for a binary mixture consisting of tagged and untagged species, both with identical M−S diffusivities $Đ_i$:

$$D_{i,self} = \frac{1}{\dfrac{1}{Đ_i} + \dfrac{\theta_i}{Đ_{ii}^{corr}}} \quad (18)$$

Since we know $Đ_i$ and $D_{i,self}$ from the MD simulations[16] of CH_4, CF_4, Ar, and Xe in MFI, the self-exchange coefficient $Đ_{ii}^{corr}$, reflecting the correlations in a single-component system, can be back-calculated. These self-exchange coefficients are shown in Figure 5a. The self-exchange coefficients follow the loading dependence

(47) Tarasenko, A. A.; Jastrabik, L.; Uebing, C. *Langmuir* **1999**, *15*, 5883.
(48) Nieto, F.; Tarasenko, A. A.; Uebing, C. *Phys. Chem. Chem. Phys.* **2000**, *2*, 3453.
(49) Bhide, S. Y.; Yashonath, S. *J. Chem. Phys.* **1999**, *111*, 1658.
(50) Bhide, S. Y.; Yashonath, S. *J. Phys. Chem. B* **2000**, *104*, 2607.

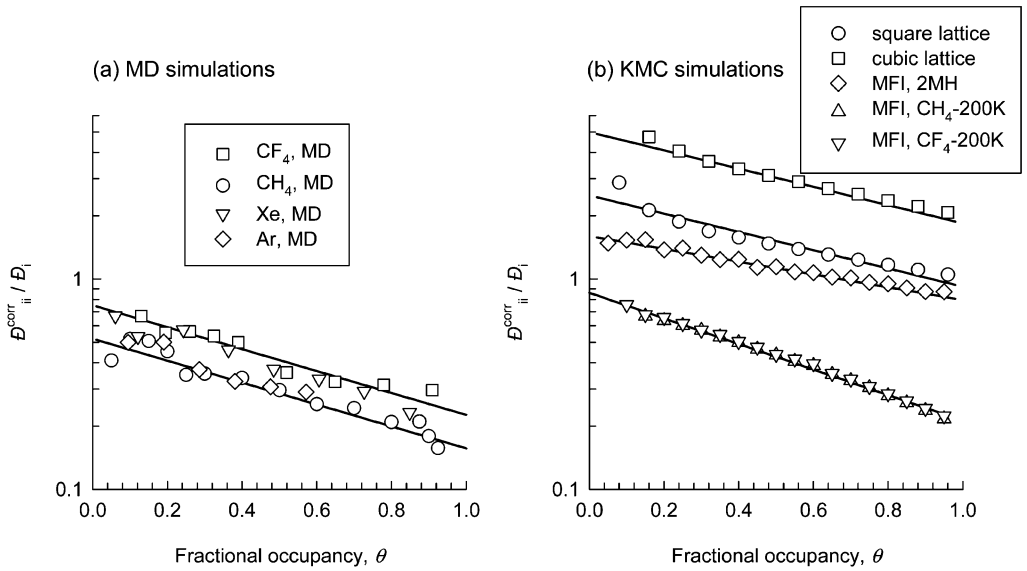

Figure 5. (a) Correlation (exchange) coefficients $Đ_{ii}^{corr}$ for the single components CH_4, CF_4, Ar, Xe, and SF_6 in MFI at 298 K as a function of fractional occupancy. Open symbols represent $Đ_{ii}^{corr}$ calculated from eq 18 from the values from MD simulation results for $Đ_i$ and $D_{i,self}$ of Skoulidas and Sholl.[16] (b) Correlation coefficients obtained from KMC simulations.[23,28,40] The continuous lines represent calculations following eq 19, along with the constants given in Table 2. In part a only the calculations for CH_4 and CF_4 are shown.

$$\frac{Đ_{ii}^{corr}}{Đ_i} = \alpha_i \exp(-\beta_i \theta) \qquad (19)$$

The fitted values of α_i and β_i in this empirical expression (eq 19) are specified in Table 2 for various molecules. It is interesting to note from Figure 5a that the $Đ_{ii}^{corr}/Đ_i$ values for CH_4 and Ar show an almost identical dependence on occupancy; both these compounds were seen earlier (cf. Figure 4a) to follow the weak confinement scenario. The molecules CF_4 and Xe, exhibiting the strong confinement scenario, yield slightly higher values of $Đ_{ii}^{corr}/Đ_i$. It appears that the degree of repulsion, or attraction, between molecules dictates $Đ_{ii}^{corr}/Đ_i$, with a higher repulsion leading to a lower exchange coefficient. The reader is referred to the papers by Bhide and Yashonath[49,50] and Uebing[47,48] for a quantitative treatment of the influence of intermolecular "interactions" in the self-diffusivities and correlations.

Topology and connectivity also affect $Đ_{ii}^{corr}/Đ_i$; to demonstrate this, we have reanalyzed the KMC simulations of Paschek and Krishna[23,28,40] for diffusion in primitive square and cubic lattices, and in MFI. The cubic lattice with the highest connectivity yields the largest values of the correlation coefficient; this is followed by the square lattice (see Figure 5b). The connectivity of MFI is significantly lower,[51] leading to lower exchange coefficients and, consequently, stronger correlation effects. The maximum number of sorption sites per unit cell of MFI is also a consideration. For 2-methylhexane (2MH), with a saturation loading $\Theta_{i,sat} = 4$, the value of $Đ_{ii}^{corr}/Đ_i$ is approximately unity; it is for this reason that Krishna and Paschek[52] suggested taking the self-exchange coefficient $Đ_{ii}^{corr}$ equal to the M−S diffusivity $Đ_i$. The KMC simulations[40] for pure components CH_4 and CF_4, with maximum capacities $\Theta_{i,sat} = 24$, yield much lower $Đ_{ii}^{corr}/Đ_i$ values; in broad agreement with the corresponding results from MD simulations (compare parts a and b of Figure 5). There are, however, *quantitative* differences in $Đ_{ii}^{corr}/Đ_i$ determined by MD and KMC simulations (compare the fit parameters listed in Table 2). These quantitative differences are attributable to the fact that intermolecular repulsions were not accounted for directly in the KMC simulations; this also explains why the values of $Đ_{ii}^{corr}/Đ_i$ are identical in the KMC simulations of CH_4 and CF_4. This is manifested in the fact that the KMC simulations modeled *both* CH_4 and CF_4 as following the strong confinement scenario.

Table 2. Fitted Constants α_i and β_i in Eq 19 for Various Components in Different Topologies

simulation type	topology	component	max. no. of molecules per unit cell or site $\Theta_{i,sat}$	α_i	β_i
MD[16]	MFI	CH_4, 298 K	20	0.52	1.2
MD[16]	MFI	CF_4, 298 K	15.4	0.75	1.2
MD[16]	MFI	Ar, 298 K	21	0.55	1.2
MD[16]	MFI	Xe, 298 K	16.5	0.7	1.2
MD[16]	MFI	SF_6, 298 K	12	0.95	1.2
KMC[28]	square	arbitrary	1	5	1
KMC[28]	cube	arbitrary	1	2.5	1
KMC[23]	MFI	2MH, 300 K	4	1.6	0.7
KMC[40]	MFI	CH_4, 200 K	24	0.86	1.4
KMC[40]	MFI	CF_4, 200 K	24	0.86	1.4

Inserting eq 19 into eq 18 allows us to estimate the self-diffusivities $D_{i,self}$ as a function of loading. These calculations agree very well with the MD simulated values for CH_4 and CF_4 (see Figure 2), as indeed they should. Due to correlation effects, the $D_{i,self}$ values are significantly lower than the corresponding values of the M−S diffusivities $Đ_i$. Only when $Đ_{ii}^{corr} \rightarrow \infty$, that is, vanishing correlations, will $D_{i,self}$ and $Đ_i$ coincide with each other.

4. Correlation Effects for Diffusion of Binary Mixtures

For binary mixtures (made up of species 1 and 2), correlation effects are embodied in the exchange coefficient

(51) Coppens, M. O.; Bell, A. T.; Chakraborty, A. K. *Chem. Eng. Sci.* **1998**, *53*, 2053.
(52) Krishna, R.; Paschek, D. *Chem. Eng. J.* **2002**, *85*, 7.

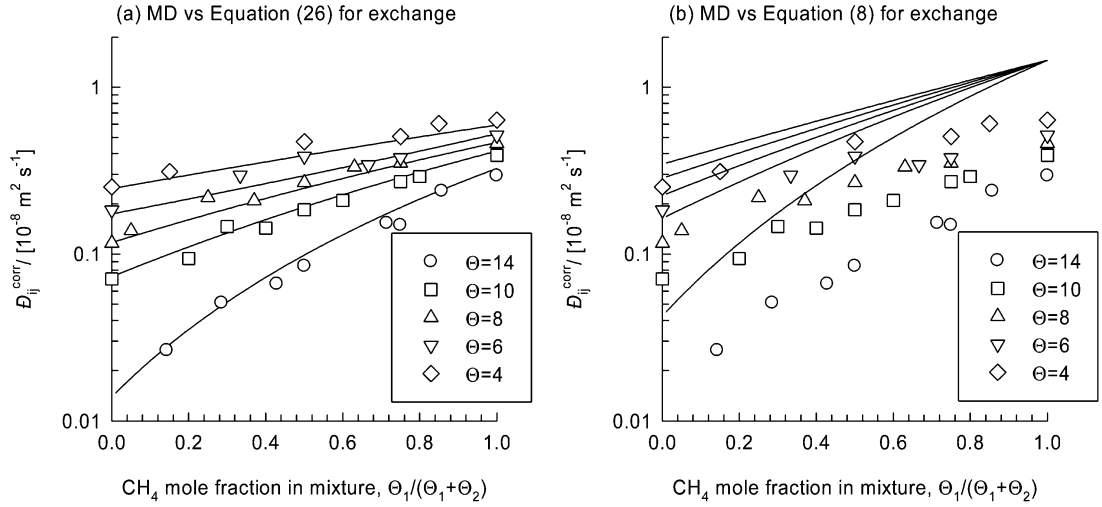

Figure 6. Correlation coefficients $Đ_{12}^{corr}$ for diffusion in CH_4/CF_4 determined from MD simulations (symbols) of [L] and eq 23. The continuous lines in part a correspond to the logarithmic interpolation formula (eq 26), along with eq 19 for $Đ_{ii}^{corr}$, as described in the text. In part b the MD results are compared with the older formula (eq 8). Note that the limiting value of $Đ_{12}^{corr}$ for $Θ_1/(Θ_1 + Θ_2) \rightarrow 0$ is $Đ_{22}^{corr}(\{Θ_{1,sat}\}/\{Θ_{2,sat}\})$; the symbols on the y-axis represent this limiting value.

$Đ_{12}^{corr}$ in the M−S formulation (eq 2). In sharp contrast to the case of single-component diffusion, these correlation effects play an integral role in the transport diffusivities, whether viewed in the M−S, Onsager, or Fick form.

To describe the diffusion of CH_4/CF_4 mixtures observed in our EMD simulations, we first determined the values of the elements of a *modified* Onsager matrix [Λ], that is linearly related to [L] and defined as follows:

$$(\mathbf{N}) = -\rho[\Theta_{sat}][\Lambda]\frac{1}{RT}(\nabla\mu) \tag{20}$$

where [Θ_{sat}] is a diagonal matrix of saturation capacities $\Theta_{i,sat}$. Recall from eq 10 that the matrix [L] can be determined directly from EMD simulations for a variety of loadings and compositions. Note that the definition of [Λ] in eq 20 is more convenient from the point of view of comparison with the M−S and Fick diffusivities, because they possess the same dimensions (m^2 s^{-1}). The modified Onsager matrix [Λ] is nondiagonal, in general, and the cross-coefficients portray the *coupling* between species diffusion.

Combining eqs 20 and 6, we obtain

$$(\mathbf{N}) = -\rho[\Lambda]\begin{bmatrix}1/\theta_1 & 0\\ 0 & 1/\theta_2\end{bmatrix}[\Gamma](\nabla\Theta) \tag{21}$$

and by comparing with eq 5, we have the following interrelationship:

$$\begin{bmatrix}\Lambda_{11} & \Lambda_{12}\\ \Lambda_{21} & \Lambda_{22}\end{bmatrix} = \begin{bmatrix}\dfrac{1}{Đ_1}+\dfrac{\theta_2}{Đ_{12}^{corr}} & -\dfrac{\theta_1}{Đ_{12}^{corr}}\\ -\dfrac{\theta_2}{Đ_{21}^{corr}} & \dfrac{1}{Đ_2}+\dfrac{\theta_1}{Đ_{21}^{corr}}\end{bmatrix}^{-1}\begin{bmatrix}\theta_1 & 0\\ 0 & \theta_2\end{bmatrix} \tag{22}$$

It is clear from eq 22 that correlations affect *all* elements of the matrix [Λ] and not just the off-diagonal ones. The expression in eq 22 allows us to determine $Đ_{12}^{corr}$ and $Đ_{21}^{corr}$ from

$$Đ_{12}^{corr} = \frac{(\Lambda_{11}\Lambda_{22} - \Lambda_{12}\Lambda_{21})}{\Lambda_{12}}; \quad Đ_{21}^{corr} = \frac{(\Lambda_{11}\Lambda_{22} - \Lambda_{12}\Lambda_{21})}{\Lambda_{21}} \tag{23}$$

For mixtures with different saturation capacities, the matrix [Λ] loses the symmetry property possessed by [L] and we obtain the following relationship for the exchange coefficients

$$\Theta_{2,sat}Đ_{12}^{corr} = \Theta_{1,sat}Đ_{21}^{corr} \tag{24}$$

The following limiting values hold for $Đ_{ij}^{corr}$:

$$\lim_{\frac{\Theta_1}{\Theta_1+\Theta_2}\rightarrow 1} Đ_{12}^{corr} \rightarrow Đ_{11}^{corr}; \quad \lim_{\frac{\Theta_1}{\Theta_1+\Theta_2}\rightarrow 1} Đ_{21}^{corr} \rightarrow Đ_{11}^{corr}\left(\frac{\Theta_{2,sat}}{\Theta_{1,sat}}\right)$$

$$\lim_{\frac{\Theta_1}{\Theta_1+\Theta_2}\rightarrow 0} Đ_{21}^{corr} \rightarrow Đ_{22}^{corr}; \quad \lim_{\frac{\Theta_1}{\Theta_1+\Theta_2}\rightarrow 0} Đ_{12}^{corr} \rightarrow Đ_{22}^{corr}\left(\frac{\Theta_{1,sat}}{\Theta_{2,sat}}\right) \tag{25}$$

The calculations of $Đ_{12}^{corr}$ from the MD simulations using eq 23 for various mixture compositions and a variety of total loadings Θ = 4, 6, 8, 10, and 14 molecules/unit cell are presented in Figure 6a. The $Đ_{12}^{corr}$ values are found to lie between those of pure CH_4 and those of pure CF_4, determined earlier from single-component diffusivity data (cf. Figure 5). The following interpolation formula

$$\Theta_{2,sat}Đ_{12}^{corr} = [\Theta_{2,sat}Đ_{11}^{corr}]^{\Theta_1/(\Theta_1+\Theta_2)}[\Theta_{1,sat}Đ_{22}^{corr}]^{\Theta_2/(\Theta_1+\Theta_2)} \tag{26}$$

is found to describe the composition dependence remarkably accurately; this relation supplants the earlier one (eq 8). To apply eq 26, we estimate $Đ_{11}^{corr}$ and $Đ_{22}^{corr}$ using eq 19, with the latter expression generalized to binary mixtures. Specifically, we replace the fractional occupancy, θ, in eq 19 with the fractional total occupancy, $(\theta_1 + \theta_2) = (\Theta_1/\Theta_{1,sat} + \Theta_2/\Theta_{2,sat})$. The M−S diffusivities in eq 19 were assumed to follow eq 12 for CH_4 and

$$Đ_2 = Đ_2(0)(1 - \theta_1 - \theta_2) \tag{27}$$

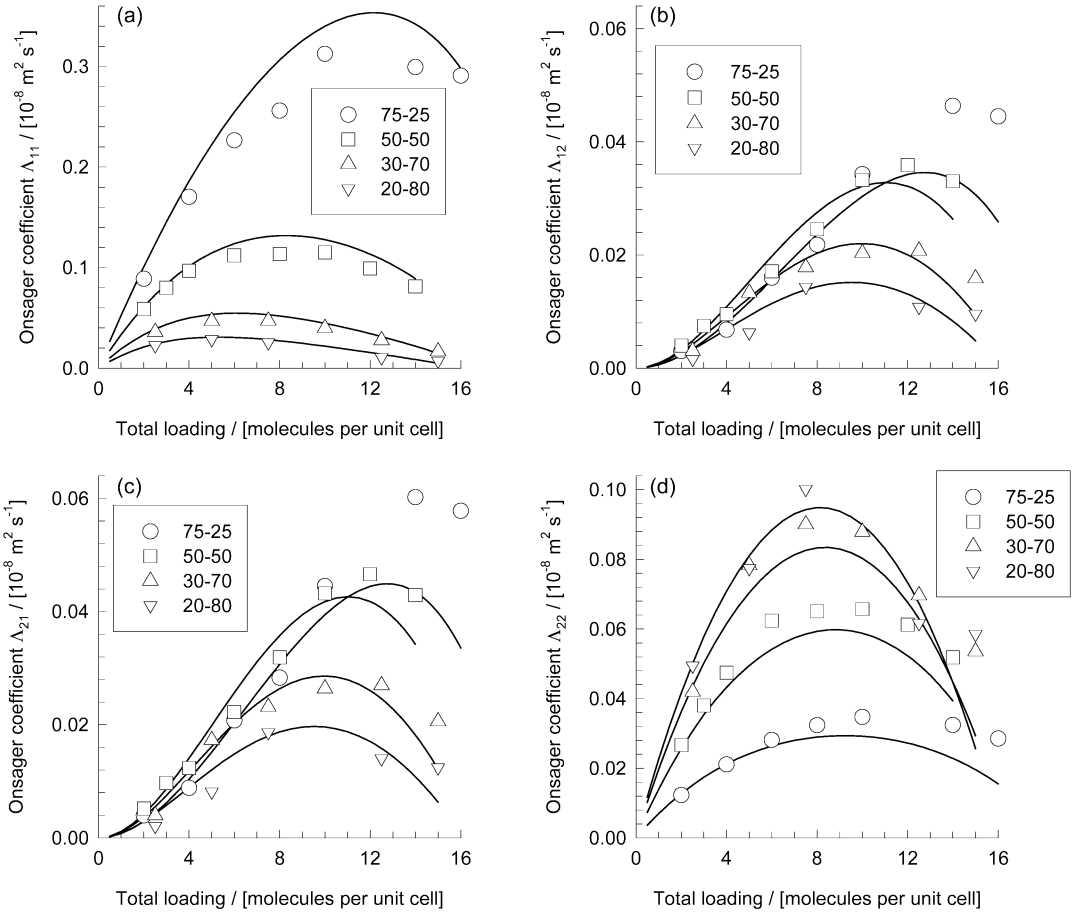

Figure 7. MD simulations (symbols) of the Onsager matrix (for 75−25, 50−50, 30−70, and 20−80 mixture compositions of CH_4/CF_4) compared with the calculations using eqs 12, 17, 19, and 26. The constants α_i and β_i are given in Table 2.

for CF_4. The latter assumption is consistent with the strong confinement scenario described above for single-component CF_4. For comparison purposes, the calculations of the exchange following eq 8 are shown in Figure 6b. The "older" formula fails to account for the strong decrease of the binary exchange coefficient with increasing loading Θ.

For the various mixtures, the M−S diffusivities $Đ_1$ and $Đ_2$, for CH_4 and CF_4, respectively, can be calculated from the MD simulated $[\Lambda]$ using eq 22; these calculations are presented in Figure 4b. We note that the $Đ_i$ values in the *mixtures* are nearly the same as those for the *pure components*; this fact underlines the major advantage of the M−S formulation of multicomponent diffusion in zeolites over the Onsager formulation for *prediction* purposes.

Equations 24 and 26 allow us to estimate the exchange coefficients $Đ_{12}^{corr}$ and $Đ_{12}^{corr}$. These coefficients used in combination with eqs 12, 27, and 22 allow us to determine the elements of $[\Lambda]$ for *binary* mixtures of CH_4 and CF_4 in MFI as a function of total loading Θ and composition. We have examined four different CH_4/CF_4 mixture compositions: 75−25, 50−50, 30−70, and 20−80. To test the accuracy of this prediction method, we present in Figure 7 a comparison of these calculations with the MD simulated values. The M−S formulation is able to describe the variation of the elements Λ_{ij} for the entire range of compositions and loadings. The success in predicting the cross-coefficients Λ_{12} and Λ_{21} is particularly noteworthy, except for high loadings approaching saturation values.

To underline the strong influence of correlation effects on *all* the elements Λ_{ij} of the Onsager matrix, we present calculations using eq 22, taking $Đ_{12}^{corr} \to \infty$. This assumption of facile (infinite) exchange yields

$$\Lambda_{12} = \Lambda_{21} = 0; \quad \Lambda_{11} = Đ_1(0)\theta_1;$$
$$\Lambda_{22} = Đ_2(0)(1 - \theta_1 - \theta_2)\theta_2 \text{ [facile exchange]} \quad (28)$$

and the corresponding calculations are shown as continuous lines in Figure 8. Also plotted in Figure 8 are the pure-component Onsager coefficients. The predictions of Λ_{11} are hopelessly in error; correlations tend to affect the more mobile CH_4 to a considerable extent and lead to a significant decrease in the Λ_{11} values, when compared to that of the pure-component value. Note also that the facile exchange scenario anticipates a monotonic increase of Λ_{11} with loading, whereas for mixtures the Λ_{11} progresses via a maximum and reduces to zero. In sharp contrast, the predictions of eq 28 for Λ_{22} are very good indeed. Arguably, these predictions are almost as good as those of the complete model with finite exchange. Correlation effects tend to have a significantly smaller effect on the mobility of the more sluggish species CF_4 than on that of the more mobile CH_4. For either CH_4 or CF_4 the Λ_{ii} cannot be identified with the pure-component values; this belies the assertion made by Sundaram and Yang[53] in developing their prediction method for the Fick matrix $[D]$.

5. Estimation of the Fick Matrix for Binary Mixtures

Once the binary M−S diffusivities have been determined, the calculation of the Fick matrix $[D]$ from eq 7

(53) Sundaram, N.; Yang, R. T. *Chem. Eng. Sci.* **2000**, *55*, 1747.

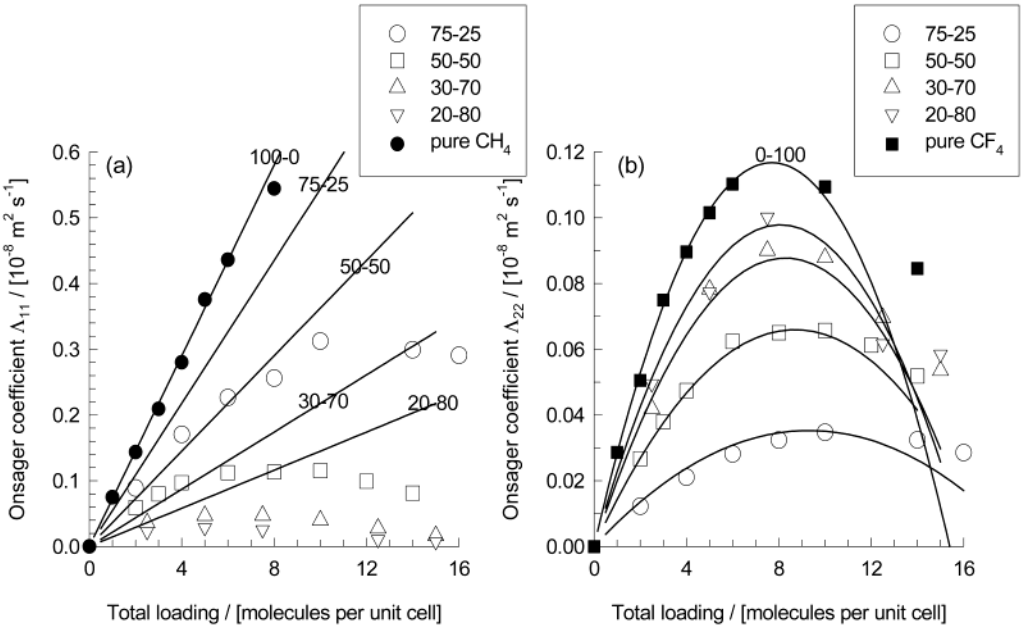

Figure 8. MD simulations (symbols) of Onsager matrix elements Λ_{11} and Λ_{22} (for the 75−25, 50−50, 30−70, and 20−80 compositions of CH_4/CF_4) compared with the calculations for facile exchange taking $Đ_{12}^{corr} \rightarrow \infty$.

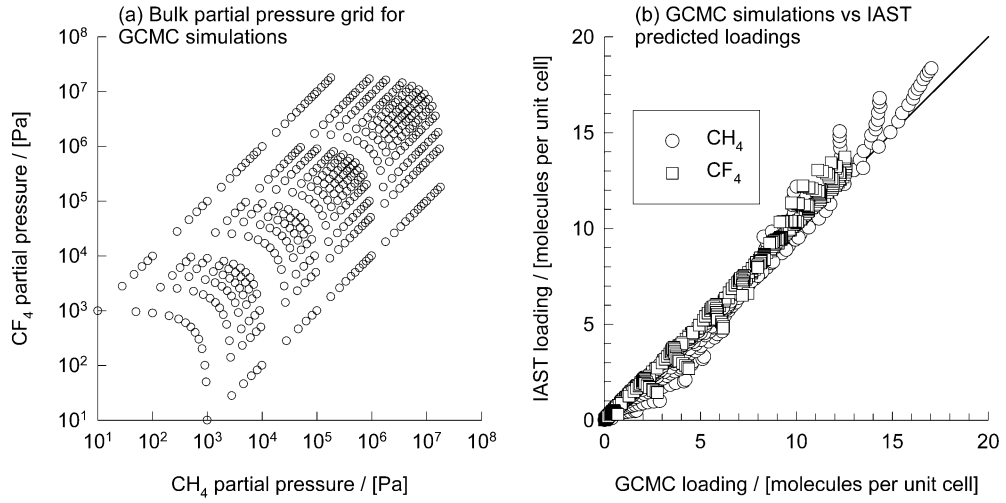

Figure 9. (a) Grid of bulk partial pressure pairs for the CH_4/CF_4 binary mixtures for which GCMC simulations were performed. (b) Parity plot between GCMC simulation data and predictions of IAST.

requires the estimation of the thermodynamic correction factor matrix [Γ]. As above, we wish to examine a means to reach this goal using only single-component data. For this purpose we use the ideal adsorbed solution theory (IAST), developed by Myers and Prausnitz,[54] that allows the estimation of the binary mixture loadings using single-component isotherm data. We first check the accuracy of the IAST predictions by comparison with GCMC simulations. A total of 454 GCMC binary mixtures' simulations were carried out for a variety of partial pressures of CH_4 and CF_4, following the grid shown in Figure 9a. Figure 9b compares the component loadings of CH_4 and CF_4 from GCMC simulations with IAST predictions based on the single-component isotherms defined in eq 15 and Table 1. The RMSDs for CH_4 and CF_4 are 0.199 and 0.099, and the agreement is generally very good except in the regions very close to saturation loadings. This point is also stressed in Figure 10, in which the component loadings are compared for (a) 70−30, (b) 50−50, and (c) 30−70 vapor mixtures as a function of the total system pressure. The deviations between IAST and GCMC are largest at very high pressures (i.e. saturation loadings).

Numerical differentiation of the IAST model equations yields the elements of Γ_{ij}, and in Figure 11 we compare the M−S model calculations, with only single-component data inputs (using eqs 6, 7, 12, 27, 22, 19, and 26), with the Fick matrix from *binary* MD simulations, along fits of *binary* GCMC simulated isotherms.[27] The agreement is generally good for the entire range of loadings and compositions. There are however some deviations between predictions and simulations at conditions approaching saturation loadings; this is due to poorer predictions of IAST under these conditions, as has already been noted above. The predictions of the M−S model assuming facile exchange (eq 28) are much poorer for D_{11} and D_{12} but reasonably good for D_{21} and D_{22} (see Figure 12). These observations are consonant with those made earlier in the context of the predictions of [Λ] using the assumption of facile exchange (cf. Figures 8 and 12).

(54) Myers, A. L.; Prausnitz, J. M. *AIChE J.* **1965**, *11*, 121.

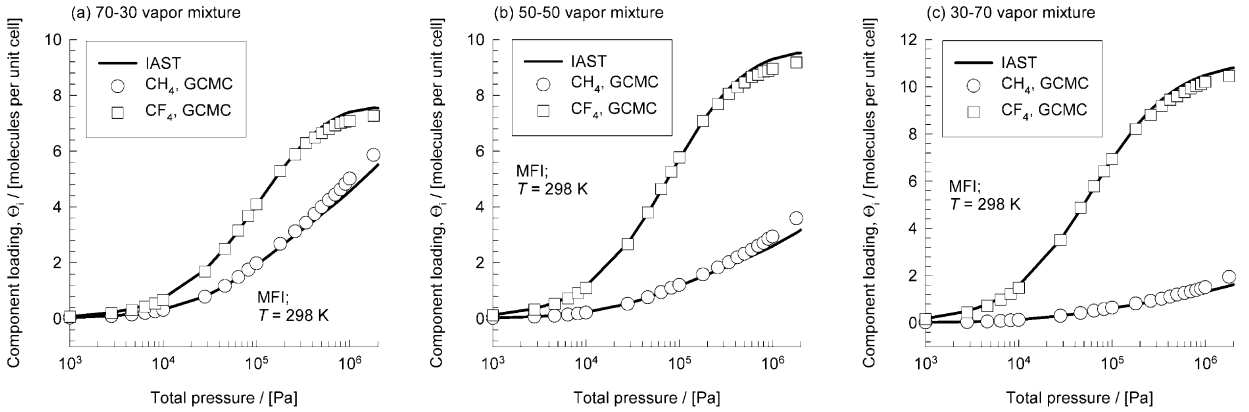

Figure 10. Component loadings in a binary mixture showing both GCMC simulations (symbols) and IAST predictions: (a) 70−30 vapor mixture; (b) 50−50 vapor mixture; (c) 30−70 vapor mixture.

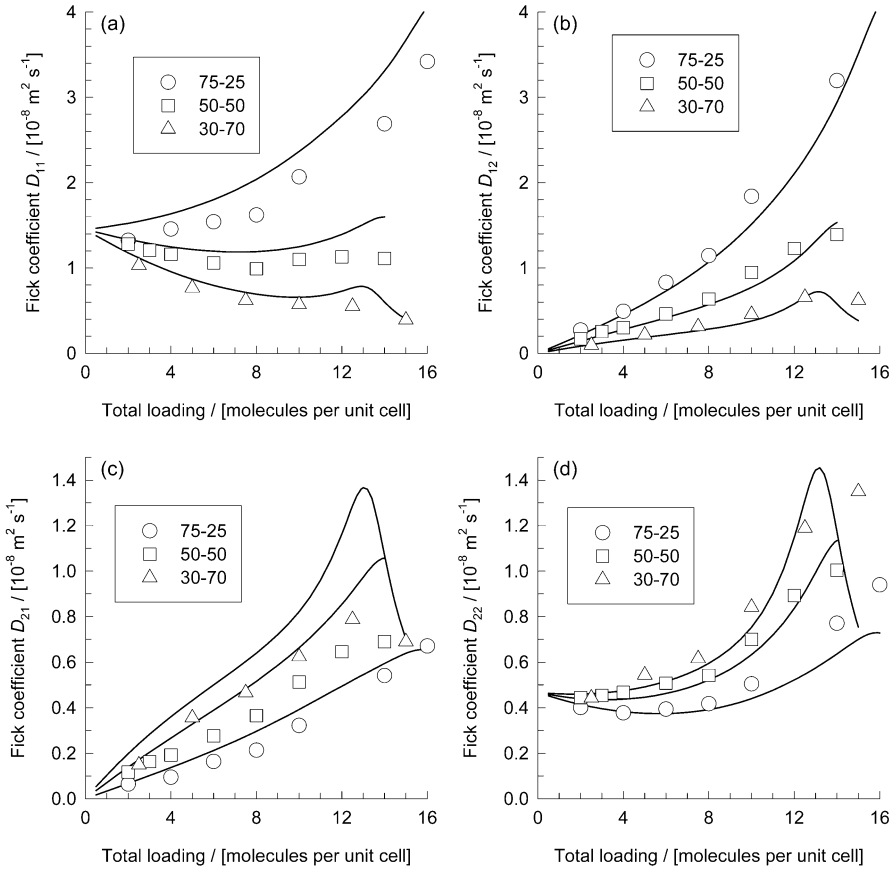

Figure 11. MD simulations (symbols) of the Fick matrix (for 75−25, 50−50, and 30−70 compositions of CH_4/CF_4) compared with the calculations using eqs 6, 7, 12, 27, 22, 19, and 26.

6. Self-diffusivities in Binary Mixtures

Often, in practice, *self*-diffusivities are determined either in theory or by experiment. Snurr and Kärger[8] performed pulsed field gradient (PFG) NMR measurements and molecular dynamics (MD) simulations to determine self-diffusivities in a mixture of CH_4 and CF_4 in MFI zeolite. Jost et al.[55] performed similar studies for mixtures of CH_4 and xenon in MFI. Gergidis et al.[9,56] studied the self-diffusivities in a mixture of CH_4 and *n*-butane in MFI using MD and quasi-elastic neutron scattering (QENS). Paschek and Krishna [34,40,57] used KMC simulations to study self-diffusivities in various mixtures and in different topologies. Schuring et al.[10] have determined the self-diffusivities in a mixture of *n*-hexane and 2-methylpentane in MFI using the tracer exchange positron emission profiling technique. Krishna and Paschek[34] derived the following expression for the self-diffusivities in a mixture of 1 and 2:

$$D_{1,\mathrm{self}} = \frac{1}{\dfrac{1}{Đ_1} + \dfrac{\theta_1}{Đ_{11}^{\mathrm{corr}}} + \dfrac{\theta_2}{Đ_{12}^{\mathrm{corr}}}}; \quad D_{2,\mathrm{self}} = \frac{1}{\dfrac{1}{Đ_2} + \dfrac{\theta_1}{Đ_{21}^{\mathrm{corr}}} + \dfrac{\theta_2}{Đ_{22}^{\mathrm{corr}}}} \tag{29}$$

(55) Jost, S.; Bar, N. K.; Fritzsche, S.; Haberlandt, R.; Karger, J. *J. Phys. Chem. B* **1998**, *102*, 6375.
(56) Gergidis, L. N.; Theodorou, D. N. *J. Phys. Chem. B* **1999**, *103*, 3380.
(57) Paschek, D.; Krishna, R. *Chem. Phys. Lett.* **2001**, *333*, 278.

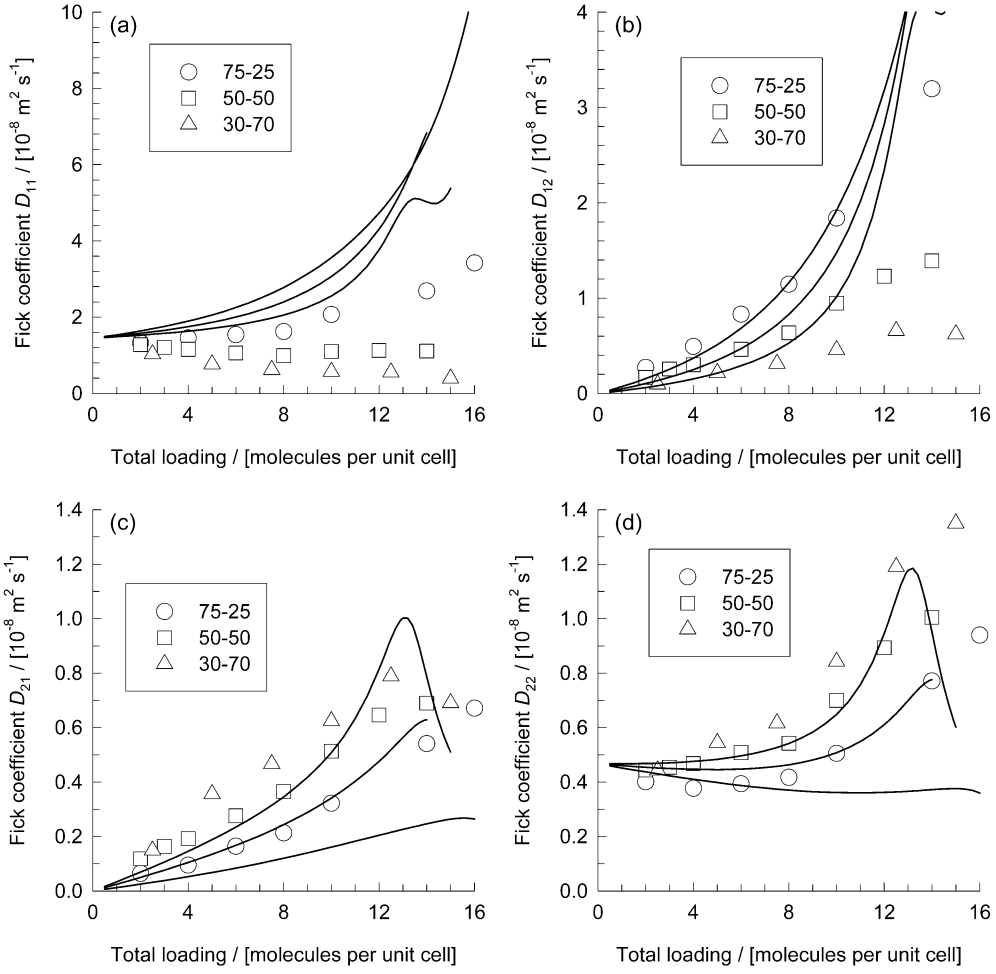

Figure 12. MD simulations (symbols) of the Fick matrix (for 75−25, 50−50, and 30−70 compositions of CH_4/CF_4) compared with the calculations for facile exchange taking $Đ_{12}^{corr} \rightarrow \infty$.

These expressions are exact, provided of course that the M−S diffusivities are known exactly. Self-diffusivities in zeolites are more strongly influenced by correlation effects associated with molecular jumps than the Onsager and Fick coefficients; this is evidenced by the fact that $D_{i,self}$ is influenced by *both* self-exchange ($Đ_{ii}^{corr}$) and binary exchange ($Đ_{12}^{corr}$). With the help of eqs 19 and 26, along with the parameter fits in Table 2, we are in a position to estimate the $D_{i,self}$ for binary mixtures.

Consider first the MD simulations of Snurr and Kärger[8] for self-diffusivities in a CH_4/CF_4 mixture in MFI at 200 K; these simulations were carried out at a total mixture loading of $\Theta = \Theta_1 + \Theta_2 = 12$, and the CH_4 loading is varied from 0 to 12 molecules per unit cell; their simulation data are shown as open symbols in Figure 13. The predictions following eq 29 are reasonably good over the whole range of compositions. In applying eq 29, the M−S diffusivities $Đ_1$ and $Đ_2$ were taken to have the same loading dependence as that determined above from simulation data at 298 K. Simulation data for the M−S diffusivities of pure CF_4 or for CH_4/CF_4 mixtures are not currently available at 200 K, but a previous study of the temperature dependence of the M−S diffusivities for pure CH_4 and pure CF_4 has indicated that the functional form of the these diffusivities with respect to loading is only very weakly affected by temperature.[15]

The KMC simulation results of Paschek and Krishna[40] for self-diffusivities in CH_4/CF_4 mixtures in MFI at 200 K for various compositions and loadings are compared in Figure 14 with the predictions of eq 29. Over the whole range of compositions and loading, the agreement with KMC simulations is very good, and it shows significant improvement over the predictions in the original publication,[40] wherein eq 8 was used for estimation of the $Đ_{12}^{corr}$.

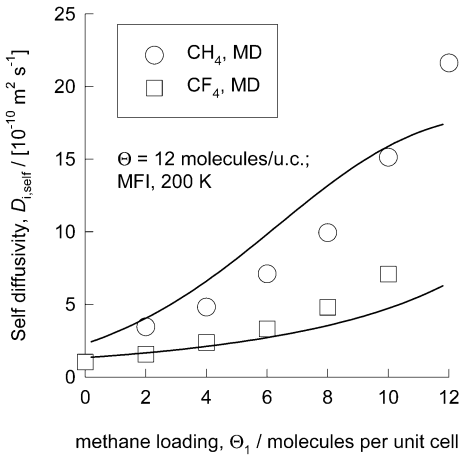

Figure 13. Comparison of MD simulations (symbols) of Snurr and Kärger[8] for self-diffusivities in a mixture of CH_4 (weakly confined) and CF_4 (strongly confined) in MFI at 200 K with calculations using eq 29. The calculations were performed taking $Đ_1(0) = 59 \times 10^{-10}$ m^2/s and $Đ_2(0) = 22 \times 10^{-10}$ m^2/s. The saturation loadings are $\Theta_{1,sat} = 20$ and $\Theta_{2,sat} = 15.4$.

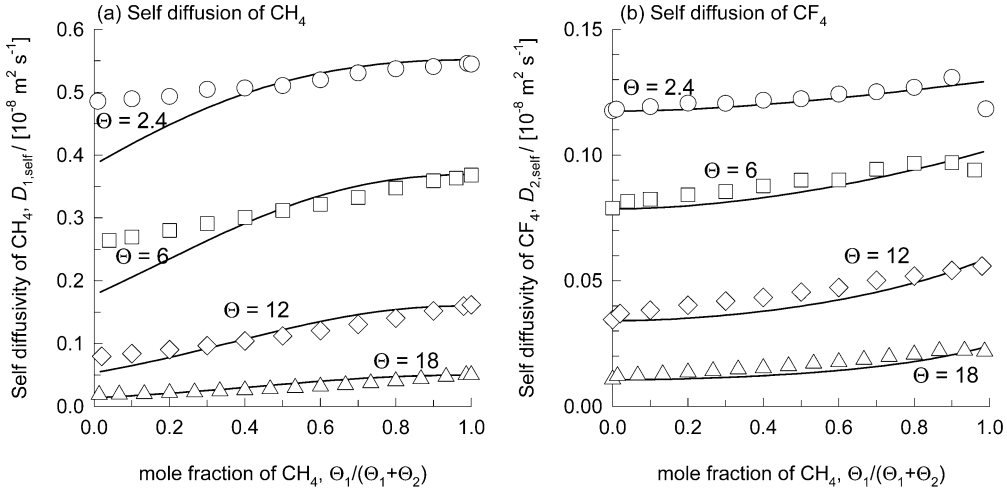

Figure 14. Comparison of KMC simulations (symbols) of Paschek and Krishna[40] for self-diffusivities in a mixture of CH_4 and CF_4 in MFI at 200 K with calculations using eq 29. The calculations were performed taking $Đ_1(0) = 69.5 \times 10^{-10}$ m²/s and $Đ_2(0) = 14.8 \times 10^{-10}$ m²/s. The saturation loadings are $\Theta_{1,sat} = \Theta_{2,sat} = 24$. Note that in the KMC simulations each of the single components follows the strong confinement scenario, and so eq 27 was used for both CH_4 and CF_4. The constants $\alpha_i = 0.86$ and $\beta_i = 1.4$, identical for both species, as indicated in Table 2.

7. Conclusions

In this investigation we have obtained new insights into correlation effects during diffusion in single-component and binary mixtures in MFI zeolite. In the M−S formulation of single-component diffusion, the correlations are captured by the self-exchange coefficient $Đ_{ii}^{corr}$. This self-exchange coefficient captures the differences that exist between the M−S and self-diffusivities for single-component systems. In earlier publications this coefficient $Đ_{ii}^{corr}$ was assumed to be equal to the single-component M−S diffusivity, $Đ_i$. A detailed analysis of single-component diffusivity data from MD and KMC simulations shows that $Đ_{ii}^{corr}/Đ_i$ is a decreasing function of the molecular loading Θ, depends on the guest−host combination, and is affected by intermolecular repulsion (attraction) forces. For different topologies $Đ_{ii}^{corr}/Đ_i$ increases with increasing connectivities. Equation 19, which is an empirical fit for the self-exchange coefficient, along with the parameters specified in Table 2, allows estimation of $Đ_{ii}^{corr}/Đ_i$. For the estimation of the M−S diffusivities $Đ_i$ in the binary mixture, due attention needs to be paid to the confinement scenario, describing the loading dependence; here too the single-component data provide adequate guidelines.

Correlations in a binary mixture are described by the binary exchange coefficient, $Đ_{12}^{corr}$. For a particular loading this binary exchange coefficient depends on the mixture composition, lying intermediate between the corresponding self-exchange ($Đ_{ii}^{corr}$) values. The logarithmic interpolation formula (eq 26) is one of the major results of this investigation. This formula provides a means to predict $Đ_{12}^{corr}$ from the pure-component self-exchange coefficients. The use of this interpolation formula in the M−S formulation, combined with the use of IAST, allows very good predictions of the Onsager and Fick coefficients and the self-diffusivities of binary mixtures of CH_4 and CF_4 in silicalite-1 using only single-component data inputs for sorption and diffusion.

The methods we have described offer a useful approximate approach to the challenging problem of quantitatively describing binary transport of sorbed species in zeolite pores. MD simulations provide an ideal complement to these approximate approaches, since MD simulations allow both the binary adsorption isotherms and the matrix of Onsager transport coefficients to be computed directly. Further MD simulations of transport in binary mixtures in zeolite topologies other than the MFI topology examined here and for adsorbed species more complex than the small, nonpolar species we have studied will be a great assistance in exploring the general validity of the approximations we have introduced.

Acknowledgment. D.S.S. was supported by a NSF CAREER award (CTS-9983647). D.S.S. is an Alfred P. Sloan fellow and a Camille Dreyfus Teacher−Scholar. R.K. acknowledges a grant from The Netherlands Foundation for Fundamental Research (NWO-CW) for the development of novel concepts in reactive separations technology.

LA034759A